Published in final edited form as:
Mol Biochem Parasitol. 2009 October ; 167(2): 135–143. doi:10.1016/j.molbiopara.2009.05.006.

A complex of three related membrane proteins is conserved on malarial merozoites

Kempaiah Rayavara[1], **Thavamani Rajapandi**[1,✧], **Kurt Wollenberg**[2], **Juraj Kabat**[3], **Elizabeth R. Fischer**[3], and **Sanjay A. Desai**[1,*]

[1]Laboratory of Malaria and Vector Research, National Institute of Allergy and Infectious Diseases, National Institutes of Health, Bethesda, Maryland, 20892, USA

[2]Bioinformatics and Computational Biosciences Branch, Office of Cyber Infrastructure and Computational Biology, National Institute of Allergy and Infectious Diseases, National Institutes of Health, Bethesda, Maryland, 20892, USA

[3]Research Technologies Branch (RTB), National Institute of Allergy and Infectious Diseases, National Institutes of Health, Bethesda, Maryland, 20892, USA

Abstract

Invasion of human red blood cells by the malaria parasite *P. falciparum* is a coordinated, multi-step process. Here, we describe three novel integral membrane proteins that colocalize on the inner membrane complex immediately beneath the merozoite plasma membrane. Each has 6 predicted transmembrane domains and is conserved in diverse apicomplexan parasites. Immunoprecipitation studies using specific antibodies reveal that these proteins assemble into a heteromeric complex. Each protein was also expressed on insect cells using the baculovirus vector system with a truncated SUMO tag that facilitates maximal expression and protein purification while permitting cleavage with SUMO protease to release unmodified parasite protein. The expressed proteins were successfully reconstituted into artificial liposomes, but were not recognized by human immune sera. Because all three genes are highly conserved in apicomplexan parasites, the complex formed by their encoded proteins likely serves an essential role for invasive merozoites.

Keywords

Apicomplexa; *Plasmodium*; merozoite; transmembrane proteins; heterologous expression

1. Introduction

The phylum Apicomplexa contains numerous unicellular parasites that are important pathogens of humans and animals, causing malaria, toxoplasmosis, and other diseases. Each member is an obligate intracellular parasite that has evolved into a specialized niche, frequently

*Corresponding author. Tel: (301) 435-7552; fax: (301) 402-2201. *E-mail address*: sdesai@niaid.nih.gov.
✧Current address: ATCC, 10801 University Blvd, Manassas VA 20110.

Competing Interests

E.R.F. is a named co-inventor on a patent application describing microwave assisted freeze substitution as used here; none of the other authors have competing interests to report.

using one or more distinct host cell types. Nevertheless, the process of invading their host cells appears to be highly conserved: both the ultrastructure and many of the implicated proteins are conserved amongst all species studied to date.

Invasion of erythrocytes by *P. falciparum*, the cause of the most virulent form of human malaria, is a complex process involving multiple receptors on the erythrocyte and a redundant collection of cognate ligands on merozoites, many of which have been identified [1,2]. After receptor-ligand interaction, a coordinated cascade of events—timed release of organelles, formation of a moving junction, de novo generation of a parasitophorous vacuole, rearward transport of surface ligands by an actively recycled actin-myosin motor complex, release of these ligands by proteases, and eventual membrane fusion—are needed to complete invasion. The actomyosin motor is sandwiched between the parasite plasma membrane and an underlying flattened vesicle known as the inner membrane complex (IMC). Beneath these layers, collectively known as the pellicle, is a specialized cytoskeleton that contains microtubule-dynein machinery and various organelles secreted at defined times during the invasion process [3–5].

While certain aspects of the invasion process are now well understood, others remain largely unexplored. For example, little is known about how the above cascade of events is coordinated or how critical information is transduced from the merozoite surface to various locations within the pellicle. Even less is known about what roles the conserved IMC may play for invasive zoites.

To address these questions and to develop a better understanding of the molecular mechanisms of invasion, it will be necessary to identify and characterize the involved proteins. The availability of genome sequence databases for various apicomplexa, microarray data that reveals genes expressed during the merozoite stage [6], and evolving informatic algorithms for predicting targeting to the invasion machinery [7,8] has created a growing list of candidate proteins for biological and physiological studies. A number of merozoite surface proteins have been identified and implicated as ligands for binding to host erythrocyte receptors. Many of these proteins are either single-transmembrane domain containing proteins or are anchored to the membrane only via glycosyl phosphatidylinositol (GPI) at their C-terminus [1,9]. GPI anchors confer segregation to detergent-resistant lipid rafts [10], may permit more rapid lateral migration in the membrane [11], allow release via the action of phospholipases [12], and permit formation of large complexes. Some of these features are well-suited for merozoite surface ligands, which must migrate to the posterior end of the merozoite with the moving junction and are often shed during invasion.

Surprisingly, only one polytopic membrane protein expressed primarily on merozoite forms has been described to date [13]. Here, we identified a highly conserved family of three genes encoding proteins with six predicted transmembrane domains. Our studies indicate that these three proteins are simultaneously expressed and that they form a heteromeric complex on the IMC. Conservation of all three proteins in distantly related apicomplexan parasites suggests expansion in a common ancestor and a critical role for invasive zoite forms.

2. Materials and Methods

2.1. Informatics and phylogenetic tree construction

A family of three paralogous genes, here named the *pfm6t* genes, was identified by searching the *P. falciparum* genome database for conserved genes encoding one or more transmembrane domains. The encoded PfM6T paralogs were aligned by the Clustal W algorithm using Vector NTI advance 10.1 (Invitrogen, Carlsbad, CA). Transmembrane domain predictions were

carried out with TMHMM 2.0 and membrane topology depictions were constructed with TOPO 2.0 (http://www.sacs.ucsf.edu/TOPO-run/wtopo.pl).

The 37 orthologous sequences were input into MUSCLE [14] to generate a multiple sequence alignment. The two M6Tβ fragments for *P. chabaudi* (PC000327.01.0 and PC000695.00.0) were combined and assigned to PC000327.01.0, the N-terminal fragment. PY06642 from *P. yoelli* appears to be a fragment of PY04760 and was excluded; PB300653.00.0 from *P. berghei* was excluded as a fragment of PB000435.02.0. The alignment was improved manually in MacVector 9.5 (MacVector, Cary, NC) and exported as a Nexus formatted file, which was used for a Bayesian phylogenetic analysis in the program MrBayes 3.1 [15]. The Bayesian phylogeny was the consensus of 7502 post-burn-in samples of two Markov chains each of which ran for 500,000 generations. The tree figure was created using FigTree (http://tree.bio.ed.ac.uk/software/figtree).

2.2. Antibodies

Peptide fragments were selected based on immunogenicity, synthesized, and KLH-conjugated for antibody production by Spring Valley Labs (Sykesville, MD). Polyclonal antibodies producing specific responses to individual PfM6T proteins were successfully raised in mice (identified with the prefix mp) and rabbits (prefix rp): KFSRYTPYPQDTNQNA-c (rp65α) for PfM6Tα; NVEMGVTENNYIKTAQY-c (rp70β and mp21β) and ARYQQTKSDWTLLHFG-c (rp68β) for PfM6Tβ; ELDIEASTENIAACKQC-c (rp64γ and mp7γ) for PfM6Tγ. A mouse monoclonal antibody for PfM6Tα was also generated using the same synthetic peptide as rp65α.

2.3. SDS-PAGE and Immunoblots

In vitro parasite cultures (Indo 1 or W2 isolates) were maintained under standard conditions, enriched by the percoll-sorbitol method [16], washed, and used for biochemical studies. Membrane and cytosolic fractions were separated by hypotonic lysis (10 mM Na_2HPO_4, pH 8.0 with 100 μg/mL PMSF, 10 μg/mL leupeptin, 2 μg/mL aprotinin, 2 μM EDTA) and ultracentrifugation at 100,000×g for 1 h at 4 °C. Peripheral proteins were extracted from the membrane pellet in some experiments with 100 mM sodium carbonate, pH 11 [17]. Protein fractions were separated on 4–12% NuPAGE gels (Invitrogen) under reducing conditions, transferred to nitrocellulose, blocked with 5% powdered milk, and probed with specific antibodies at 1:5000-1:1000 dilutions. A rabbit polyclonal antibody against the SUMO tag of expressed proteins was used at a 1:500 dilution (Life Sensors, Malvern, PA). For detection of immune responses against PfM6T proteins, Ni-NTA purified proteins expressed in insect cells were probed with pooled human serum (1:2000 dilution) from 10 healthy adults living in endemic sites in Mali or Cambodia. These sera were provided by Dr. Rick Fairhurst and were collected with written informed consent under an NIAID IRB-approved protocol. After extensive washing, blots were incubated with HRP-conjugated goat anti-mouse, anti-rabbit, or anti-human IgG (Jackson ImmunoResearch Laboratories, West Grove, PA) at a dilution of 1:10,000 for 1h, washed, and visualized using SuperSignal West Pico substrate (Pierce, Rockford, IL).

For stage specificity analysis of PfM6T expression, *in vitro* cultures were synchronized with 2 consecutive incubations in 5% sorbitol and cultured for indicated durations before harvesting for immunoblotting of matched samples.

2.4. Immunoprecipitation

Antibodies (rp65α, rp70β and mp7γ) were separately cross-linked to Dynabeads protein A (Invitrogen) according to the manufacturer's protocol. Infected cell lysate in 0.1M Na_2HPO_4, pH 8.0 with 1% CHAPS, 100 μg/mL PMSF, 10 μg/mL leupeptin, 2 μg/mL aprotinin was

incubated with these beads or with control beads without crosslinking for 30 min before washing extensively and elution by boiling in loading buffer for immunoblot analysis.

2.5. Indirect immunofluorescence confocal microscopy

Indirect immunofluorescence assays (IFA) were performed as described [18]. Briefly, synchronous cultures of infected erythrocytes were washed to remove serum before making thin smears on glass slides. The cells were air dried, fixed in 1% freshly prepared paraformaldehyde in PBS, washed, and blocked with 5 mg/ml goat serum and 0.1% triton X-100 in PBS. Primary and secondary antibodies were applied in the same buffer at a dilution of 1:100 and incubated at 37 °C for 1hr with extensive washing between antibodies. Colocalization studies used two primary antibodies applied simultaneously. Antibodies against known merozoite surface proteins were mouse monoclonal antibodies against a 42 kD fragment of MSP-1 (R9256/EcMSP-1_{42}) and AMA-1 (4H9/19), both kindly provided by Dr. Sanjay Singh. Species-specific secondary antibodies coupled to fluoropores were used to detect the distribution of these antigens. Goat anti-mouse or anti-rabbit IgGs conjugated to either Alexa Fluor-488 (green) or Alexa Fluor-594 (red) were obtained from Invitrogen. Where shown, nuclear staining was with 300 nM 4, 6-diamidino-2-phenylindole (DAPI). Slides were mounted with Vectashield (Vector Laboratories, Burlingame, CA) and visualized on a Leica SP2 laser scanning confocal microscope (Leica Microsystems, Exton, PA) under a 68x oil immersion objective. Images were processed in Imaris 6.0 (Bitplane AG, Zurich, Switzerland) and uniformly deconvolved using Huygens Essential 3.1 (Scientific Volume Imaging BV, Hilversum, The Netherlands). *x-y* plots showing positional fluorescence intensity along the parasite's apical-posterior axis were also created in Huygens Essential 3.1 and exported to SigmaPlot 10.0 (Systat, San Jose, CA).

2.6. Immunoelectron microscopy

Infected erythrocytes fixed overnight at 4 °C with 0.075% glutaraldehyde/4 % paraformaldehyde were suspended in Hanks buffered saline solution with 10% BSA. 1.5 μl were aliquoted to "hats" (Leica Microsystems, Vienna, Austria) for cryo-immobilization in a Leica EMPact2. Freeze substitution with 1% uranyl acetate/0.1% glutaraldehyde in acetone and dehydration was performed with microwave irradiation (Pelco 3451 microwave processor, 8 cycles of 2 min on–2 min off–2 min on; Ted Pella, Redding, CA) at −78 °C and embedded in LR white resin. Thin sections were cut using an MT-7000 ultramicrotome (Ventana, Tucson, AZ), etched with 4% meta-periodate, and immunolabeled in a Pelco 3451 microwave oven using a Pelco PFTE immunostaining pad. After blocking with 1% BSA/0.1% Tween 20 Tris buffer for 2 min at 150 Watts/24° C (additional steps retained same settings), samples were incubated with primary antibody for 2 × 2 min, washed 3 × 1 min, incubated with secondary 5 nm colloidal gold (BBInternational, Cardiff, UK) for 2 × 2 min before final rinsing. Sections were stained with 1% uranyl acetate and viewed on a Philips CM-10 TEM (FEI, Hillsboro, OR) at 80 kV. Images were acquired with a Hammamatsu XR-100 digital camera system (AMT, Danvers, MA.)

For pre-embed labeling with antibodies, specimens were fixed with 2% paraformaldehyde with 0.0075% glutaraldehyde for 30min, blocked with 10% goat serum for 1 hr, and incubated with rabbit primary antibodies for 1 hr followed by goat anti-rabbit antibody conjugated to 10 nm colloidal gold (BBI International, Cardiff, UK). They were then washed and incubated in 2% paraformaldehyde/0.0075% glutaraldehyde overnight at 4 °C, washed in distilled H_2O, dehydrated in ethanol before embedding, sectioning, and staining as above.

2.7. Cloning, baculovirus production, and insect cell expression

The full-length transcript for each paralog was amplified from parasite cDNA with the following primers: GCGGTCTCGAGGTATGTGGTTTACA and

GCGAGCTCTTAAGCTGGATAAT (forward and reverse primers, respectively, for PfM6Tα with engineered BsaI and SacI sites underlined), GCGGTCTCGAGGTATGGGTTCAT and GCGAGCTCTCAATATTGAGCTGT (PfM6Tβ with BsaI and SacI sites), GCGGTCTCGAGGTATGTTTTTTACTTA and GCGGATCCTTAACATTGTTTGCA (PfM6Tγ with BsaI and BamHI sites). Each amplicon was digested with BsaI to produce a sense strand 5' overhang complimentary to an ACCT antisense strand overhang in the iCTHS vector (Life Sensors, Malvern, PA, USA). Ligation into this vector then created a single open reading frame encoding a 6-histidine tag (6-His) followed by a half-SUMO tag (CTHS) immediately upstream of the *pfm6t* gene. After cloning and confirming sequence, each plasmid was recombined into an expression bacmid as described (Bac-to-Bac baculovirus expression system, Invitrogen, Carlbad, CA, USA). Successful transformation was selected with 50 μg/mL kanamycin, 7 μg/mL gentamicin, 10 μg/mL tetracycline, and 100 μg/mL Bluo-gal (Technova, Hollister, CA, USA); recombinants were selected with blue-white screening using IPTG, sequenced to exclude mutations, and subjected to bacmid harvest for transfection of *Spodoptera frugiperda* (Sf9) insect cells with Cellfectin (Invitrogen). After a 72 h incubation at 28 °C, baculovirus released into the supernatant was harvested, used to confirm the gene's presence by PCR, and passaged further in Sf9 or *Trichopulsia ni* (High Five cells, Invitrogen). Viral titers were determined by plaque assays with Neutral Red (Invitrogen). Expressed protein was harvested from suspension cultures using recombinant baculovirus at a multiplicity of infection (MOI) of 10 and a 72 h incubation at 28 °C.

Indirect immunofluorescence confocal microscopy was performed using a sterile chamber with a coverglass bottom with adherent insect cells transfected with baculovirus at a MOI of 3 and fixation in 1% paraformaldehyde before labeling.

2.8. Ni^{2+}-NTA purification of expressed protein

Transfected *T. ni* cells were suspended in 25 volumes of 50 mM tris-HCl (pH 7.5) with 250 mM sucrose, 20 mM β-mercaptoethanol, 100 μg/mL PMSF, 10 μg/mL leupeptin, 2 μg/mL aprotinin and 20 μg/mL DNase, and subjected to 3 freeze-thaw cycles with sonication. Membranes were then isolated by ultracentrifugation (100,000 × *g*, 1 h at 4 °C) before solubilization in 50 mM Na_2HPO_4 buffer at pH 7.0 containing 8 M urea, 1 % CHAPS, 1 % n-dodecyl-β-D-maltoside and 1 % n-octyl-β-D-glucoside with a dounce homogenizer. After removing insoluble material by ultracentrifugation, solubilized proteins were subjected to Ni^{2+}-NTA purification using the ProBond Purification System (Invitrogen). 6-His tagged proteins were allowed to bind to the column under continuous agitation for 12 h, washed with 10 mM imidazole, pH 6.0 in the above buffer, and eluted in the buffer with 200 mM imidazole, pH 4.0.

2.9. Reconstitution into liposomes and SUMO protease digestion

Soybean azolectin (lecithin, type II; Sigma Aldrich, St. Louis, MO) was sonicated at 4 mg lipid /ml in 40 mM tris-HCl (pH 7.5) with 4 mM DTT and 0.2 mM EDTA to homogenity. Ni^{2+}-NTA purified protein reconstituted into liposomes by mixing with this lipid and extensive dialysis against 50 mM Na_2HPO_4, pH 7.0 with methanol-washed SM2 Bio-Beads (Bio-Rad, Hercules, CA). A 50 μl liposome suspension in PBS was incubated with 20 μg N-terminal half SUMO (NTHS, Life Sensors) for 30 min at 30 °C with intermittent sonication before addition of 40 units SUMO protease (Life Sensors) with 2 mM DTT. The mixture was incubated overnight at 4 °C to permit specific cleavage of the chimeric protein. This technology is designed to prevent CTHS cleavage by endogenous SUMO proteases in insect cells, but allow cleavage by exogenous SUMO protease after protein purification because association of NTHS with CTHS restores protease sensitivity. This cleavage yields unmodified, full length PfM6T protein without the 6-His-CTHS tag.

3. Results

3.1. Identification and conservation of the M6T gene family

We searched the annotated *P. falciparum* genome database (www.plasmodb.org) for predicted membrane proteins unique to protozoan parasites and identified a sizeable collection including PF14_0065, a 2 intron-containing gene on chromosome 14. We were interested in this gene because we had also identified its product through LC/MS sequencing of membrane proteins harvested from blood-stage cultures (data not shown). Two related, but distinct genes were evident on chromosomes 4 and 13 (PFD1110w and MAL13P1.130, respectively.) All three gene products are of similar size (284–372 residues) and have six predicted transmembrane domains, permitting us to create a graphical representation of their membrane topology and high degree of conservation (Fig. 1A). This figure reveals conservation of these paralogs both within and between predicted transmembrane domains. Table 1 lists pairwise sequence comparisons and timing of transcription for each gene based on genome-wide expression surveys. We named these putative proteins PfM6Tα (PF14_0065), PfM6Tβ (PFD1110w), and PfM6Tγ (MAL13P1.130) using an acronym for "merozoite 6 transmembrane" based on data described below.

Each gene product is conserved in other plasmodial species as well as more distantly related apicomplexan parasites (Figs. 1B and supplementary Fig. S1). Despite high-level conservation between the *P. falciparum* paralogs (Fig. 1A), our analysis revealed unambiguous separation into three distinct orthologous clades. These clades, corresponding to the three paralogs in *P. falciparum*, have posterior probabilities of 1.0, 1.0, and 0.99, indicating statistically significant separation between them. In each clade, the *Cryptosporidium* genes occupy an ancestral position, followed by a group consisting of *Toxoplasma gondii* sequences and an interior group for sequences from *Plasmodia*, *Theileria*, and *Babesia*. The significant posterior probabilities of each clade suggest that three paralogous copies existed in an ancestral apicomplexan and that each has been carried through the evolution of these parasites. Expansion of this family may be ongoing as *T. gondii* appears to have an extra copy of M6Tγ.

3.2. Localization with specific antibodies against each protein

We next raised polyclonal antibodies using synthetic peptides that match regions of each predicted *P. falciparum* protein but absent from the other two paralogs (see Methods and Fig. S2). These antibodies were first used in confocal immunofluorescence microscopy to localize these three proteins. With each antibody, maximal fluorescence intensity was observed on late-stage schizonts ("segmenters") and freed merozoites (Fig. 2). The labeling was primarily on the surface of each daughter cell; its pattern did not significantly change upon erythrocyte rupture and release of invasive merozoites (Fig. 2, bottom row). Double-labeling with paralog-specific antibodies revealed that these three proteins colocalize with each other. In contrast, they do not colocalize well with MSP-1, an extensively studied merozoite plasma membrane antigen [19] (Fig. 3A and 3B). Quantification of fluorescence intensities along the apical-posterior axis of merozoites suggested that MSP-1's location is external to that of each paralog (Fig. 3B). We also noticed that colocalization studies with AMA-1, a surface antigen restricted to the merozoite apical end [20], consistently revealed a reduced signal for PfM6Tα at the apical end of each merozoite (Fig. 3C).

To more rigorously examine these differences, immuno-electron microscopy was performed with antibodies against PfM6Tα and MSP-1 antibodies (Fig. 4A and B, respectively). Antibody labeling prior to embedding and sectioning of specimens yielded strong labeling with anti-MSP-1, but no labeling with anti-PfM6Tα. This suggests MSP-1 is accessible on the surface of merozoites without membrane permeabilization, but that PfM6Tα is not. Embedding and sectioning of specimens yielded labeling with both antibodies and indicated that PfM6Tα is

on the IMC while MSP-1 is on the merozoite plasma membrane. Because PfM6Tα co-precipitates with each of the other paralogs (see below), we infer that all three are targeted to the IMC.

3.3. Timing of expression and immunoprecipitation studies

The specificity of each antibody was further evaluated with immunoblots. Antibodies against specific epitopes on PfM6Tα, PfM6Tβ, and PfM6Tγ each recognized a single protein in infected erythrocyte lysate migrating at 28, 42, and 30 kDa, consistent with predicted molecular weights of 33, 43, and 34 kDa, respectively (lane 1 in each group, Fig. 5A). In each case, ultracentrifugation confirmed association with the membrane fraction (lane 2), consistent with 6 predicted transmembrane domains, though PfM6Tγ unexpectedly also partitions to the soluble fraction. Importantly, none of these antibodies appears to cross react with the other two paralogs because only a single band was detected with each antibody. (See additional evidence using heterologous expression of individual paralogs below.)

In light of their markedly similar sequences and similarly regulated expression on merozoites (Fig. 5B and Table 1), we wondered if the three paralogs assemble into a heteromeric complex. We evaluated this possibility with immunoprecipitation from non-denaturing detergent-solubilized lysate. After conjugating to protein A beads, antibodies to either PfM6Tβ or PfM6Tγ successfully retrieved PfM6Tα, whereas beads not conjugated to antibodies failed to retrieve this protein (Fig. 5C, first group). PfM6Tβ was similarly retrieved by antibodies to the other two paralogs (second group). None of these antibodies were able to capture the merozoite's rhoptry-associated protein 1 (RAP1), excluding formation of non-specific complexes.

3.4. Heterologous expression and reconstitution of each PfM6T protein

Our attempts to express these proteins in *Xenopus* oocytes and in bacteria were unsuccessful, possibly because of *P. falciparum*'s unusual codon usage or more universal difficulties of membrane protein expression. High level expression of each paralog was instead achieved using baculovirus-infected insect cells [21] after we engineered a fusion tag with the C-terminal half of SUMO (CTHS) at the N-terminus of each PfM6T protein (Fig. 6A). This tag improves translation of full-length proteins, increase protein stability, and can be cleaved off with SUMO-specific proteases after harvest to liberate unmodified native protein [22]. We also included a 6-His motif in this N-terminal tag to facilitate affinity purification on metal chelation columns.

Robust expression in *S. frugiperda* (Sf9) insect cells was detected with both PfM6T-specific and anti-SUMO antibodies 72 h after transfection of bacmid carrying each tagged PfM6T construct (Fig. 6B), whereas untransfected Sf9 cell extracts were not recognized. None of the singly transfected cells were recognized by antibodies against either of the other paralogs, definitively confirming antibody specificity. Each expressed protein migrated at approximately a 6 kDa higher molecular weight than its native parasite protein, consistent with addition of the 6-His-CTHS tag. A ~28 kDa fragment was also apparent in immunoblots using PfM6Tβ-transfected cell extracts. It is not clear whether this represents a degradation product or synthesis of a truncated product.

Baculovirus for each construct was harvested and transfected into a *Trichoplusia ni* insect cell line, which frequently achieves higher level expression than Sf9 cells. With both cell types, we detected robust expression in IFA experiments (not shown). We used the *T. ni* expression system to affinity purify each expressed protein on nickel-chelating resin (Ni^{2+}-NTA) via affinity for the N-terminal 6-His tag. Purified protein reconstituted preferentially into membranes of liposomes formed by detergent removal, confirming that these proteins are

capable of spontaneous incorporation in the lipid bilayers (Fig. 6C). Treatment of reconstituted protein with SUMO protease was able to release the 6-His-CTHS tag to generate protein with an unmodified primary sequence (Fig. 6D).

Enrichment of PfM6T proteins from a heterologous expression system permits their characterization without confounding effects from other parasite proteins. With this in mind, the Ni^{2+}-NTA purified protein was also used to evaluate human immune responses to PfM6T proteins with pooled sera from human subjects in Mali and Cambodia. Neither pool recognized any of the 3 recombinant PfM6T proteins, suggesting that these proteins do not elicit a significant immune response (not shown). Control immunoblots using infected erythrocytes revealed multiple bands recognized by these sera that are not detected on uninfected erythrocytes.

4. Discussion

The *pfm6t* genes represent a novel highly conserved gene family that encodes 3 simultaneously expressed polytopic membrane proteins. These genes are not subject to gene-silencing and monoallelic expression of one paralog, as has been observed for a number of other gene families in *P. falciparum* [23–26]. Although each corresponding protein is maximally expressed on merozoites, they lack N-terminal signal sequences implicated in targeting to the merozoite surface or apical organelles [7,8]. Instead, our immuno-electron microscopy experiments reveal that these proteins are targeted to the IMC and have distributions distinct from those of well-studied antigens such as MSP-1 and AMA-1. Based on multiple pairwise immunoprecipitation experiments, the three M6T proteins then appear to form stable interactions with each other.

Successful expression of these proteins with a cleavable 6-His-CTHS tag in baculovirus-infected cells permitted us to partially purify expressed protein. It also provided direct biochemical evidence for their membrane association by liposome reconstitution, demonstrated that SUMO protease can be used to specifically remove engineered tags from expressed protein, and revealed that these proteins do not elicit lasting immunity through natural infections. These insights were possible without optimization away from *P. falciparum*'s atypical codon usage and despite the presence of 6 predicted transmembrane domains in each protein. Reconstitution of the native heterocomplex from these individually expressed members is being explored and may help determine its function. With ongoing advances in baculovirus transfection technology, it may also be possible to express all three paralogs in a single insect cell simultaneously [27]. Expression in insect cells, possibly with a SUMO tag designed to facilitate expression, should be considered for other refractory *P. falciparum* proteins.

Because our immunoprecipitation data implicate stable interactions between these proteins, they appear to form a heteromeric complex with at least 18 transmembrane domains based on a simple 1:1:1 subunit stoichiometry; complicated stoichiometries or association with other yet unidentified membrane proteins may yield additional transmembrane domains. What might be the role of this conserved membrane complex? We speculate that it may function in signal transduction or transmembrane solute transport across one or both membranes of the IMC. If the complex does mediate ion or solute transport, the role of the IMC may be to store these solutes near the merozoite surface for rapid access upon initiation of host cell invasion.

Our study along with recent proteomic and molecular biological studies are providing new targets for clinical intervention in malaria and other diseases caused by apicomplexan parasites. While zoite invasion has long been seen as an Achilles heel because the parasite is not sequestered within a host cell, research has been largely directed toward development of a

vaccine that blocks invasion. As this has not proven fruitful, it may be time to consider development of chemotherapeutic agents that specifically target the complex and coordinated intracellular events needed within the zoite to complete invasion.

Supplementary Material

Refer to Web version on PubMed Central for supplementary material.

Acknowledgments

We thank Jose Riberio for help with bioinformatics, Sanjay Singh and Rick Fairhurst for providing antibodies and human immune sera, and Owen Schwartz and Meggan Czapiga for help with confocal microscopy and deconvolution of images. This research was supported by the Intramural Research Program of the National Institutes of Health, National Institute of Allergy and Infectious Diseases.

References

1. Gaur D, Mayer DC, Miller LH. Parasite ligand-host receptor interactions during invasion of erythrocytes by Plasmodium merozoites. Int J Parasitol 2004;34:1413–1429. [PubMed: 15582519]
2. Cowman AF, Crabb BS. Invasion of red blood cells by malaria parasites. Cell 2006;124:755–766. [PubMed: 16497586]
3. Morrissette NS, Sibley LD. Cytoskeleton of apicomplexan parasites. Microbiol Mol Biol Rev 2002;66:21–38. [PubMed: 11875126]
4. Kappe SH, Buscaglia CA, Bergman LW, et al. Apicomplexan gliding motility and host cell invasion: overhauling the motor model. Trends Parasitol 2004;20:13–16. [PubMed: 14700584]
5. Aikawa M, Miller LH, Johnson J, et al. Erythrocyte entry by malarial parasites. A moving junction between erythrocyte and parasite. J Cell Biol 1978;77:72–82. [PubMed: 96121]
6. Llinas M, Bozdech Z, Wong ED, et al. Comparative whole genome transcriptome analysis of three *Plasmodium falciparum* strains. Nucleic Acids Res 2006;34:1166–1173. [PubMed: 16493140]
7. Treeck M, Struck NS, Haase S, et al. A conserved region in the EBL proteins is implicated in microneme targeting of the malaria parasite *Plasmodium falciparum*. J Biol Chem 2006;281:31995–32003. [PubMed: 16935855]
8. Ghoneim A, Kaneko O, Tsuboi T, et al. The *Plasmodium falciparum* RhopH2 promoter and first 24 amino acids are sufficient to target proteins to the rhoptries. Parasitol Int 2007;56:31–43. [PubMed: 17175193]
9. Sanders PR, Gilson PR, Cantin GT, et al. Distinct protein classes including novel merozoite surface antigens in Raft-like membranes of *Plasmodium falciparum*. J Biol Chem 2005;280:40169–40176. [PubMed: 16203726]
10. Brown DA. Interactions between GPI-anchored proteins and membrane lipids. Trends Cell Biol 1992;2:338–343. [PubMed: 14731512]
11. Ishihara A, Hou Y, Jacobson K. The Thy-1 antigen exhibits rapid lateral diffusion in the plasma membrane of rodent lymphoid cells and fibroblasts. Proc Natl Acad Sci USA 1987;84:1290–1293. [PubMed: 2881297]
12. Englund PT. The structure and biosynthesis of glycosyl phosphatidylinositol protein anchors. Annu Rev Biochem 1993;62:121–138. [PubMed: 8352586]
13. O'Donnell RA, Hackett F, Howell SA, et al. Intramembrane proteolysis mediates shedding of a key adhesin during erythrocyte invasion by the malaria parasite. J Cell Biol 2006;174:1023–1033. [PubMed: 17000879]
14. Edgar RC. MUSCLE: multiple sequence alignment with high accuracy and high throughput. Nucleic Acids Res 2004;32:1792–1797. [PubMed: 15034147]
15. Ronquist F, Huelsenbeck JP. MrBayes 3: Bayesian phylogenetic inference under mixed models. Bioinformatics 2003;19:1572–1574. [PubMed: 12912839]

16. Aley SB, Sherwood JA, Howard RJ. Knob-positive and knob-negative *Plasmodium falciparum* differ in expression of a strain-specific malarial antigen on the surface of infected erythrocytes. J Exp Med 1984;160:1585–1590. [PubMed: 6208311]

17. Fujiki Y, Hubbard AL, Fowler S, et al. Isolation of intracellular membranes by means of sodium carbonate treatment: application to endoplasmic reticulum. J Cell Biol 1982;93:97–102. [PubMed: 7068762]

18. Kaneko O, Fidock DA, Schwartz OM, et al. Disruption of the C-terminal region of EBA-175 in the Dd2/Nm clone of *Plasmodium falciparum* does not affect erythrocyte invasion. Mol Biochem Parasitol 2000;110:135–146. [PubMed: 10989151]

19. Miller LH, Roberts T, Shahabuddin M, et al. Analysis of sequence diversity in the *Plasmodium falciparum* merozoite surface protein-1 (MSP-1). Mol Biochem Parasitol 1993;59:1–14. [PubMed: 8515771]

20. Peterson MG, Marshall VM, Smythe JA, et al. Integral membrane protein located in the apical complex of *Plasmodium falciparum*. Mol Cell Biol 1989;9:3151–3154. [PubMed: 2701947]

21. Kost TA, Condreay JP, Jarvis DL. Baculovirus as versatile vectors for protein expression in insect and mammalian cells. Nat Biotechnol 2005;23:567–575. [PubMed: 15877075]

22. Butt TR, Edavettal SC, Hall JP, et al. SUMO fusion technology for difficult-to-express proteins. Protein Expr Purif 2005;43:1–9. [PubMed: 16084395]

23. Chen Q, Fernandez V, Sundstrom A, et al. Developmental selection of var gene expression in *Plasmodium falciparum*. Nature 1998;394:392–395. [PubMed: 9690477]

24. Kyes SA, Rowe JA, Kriek N, et al. Rifins: a second family of clonally variant proteins expressed on the surface of red cells infected with *Plasmodium falciparum*. Proc Natl Acad Sci USA 1999;96:9333–9338. [PubMed: 10430943]

25. Fernandez V, Hommel M, Chen Q, et al. Small, clonally variant antigens expressed on the surface of the *Plasmodium falciparum*-infected erythrocyte are encoded by the rif gene family and are the target of human immune responses. J Exp Med 1999;190:1393–1404. [PubMed: 10562315]

26. Niang M, Yan YX, Preiser PR. The *Plasmodium falciparum* STEVOR multigene family mediates antigenic variation of the infected erythrocyte. PLoS Pathog 2009;5:e1000307. [PubMed: 19229319]

27. Belyaev AS, Roy P. Development of baculovirus triple and quadruple expression vectors: co-expression of three or four bluetongue virus proteins and the synthesis of bluetongue virus-like particles in insect cells. Nucleic Acids Res 1993;21:1219–1223. [PubMed: 8385313]

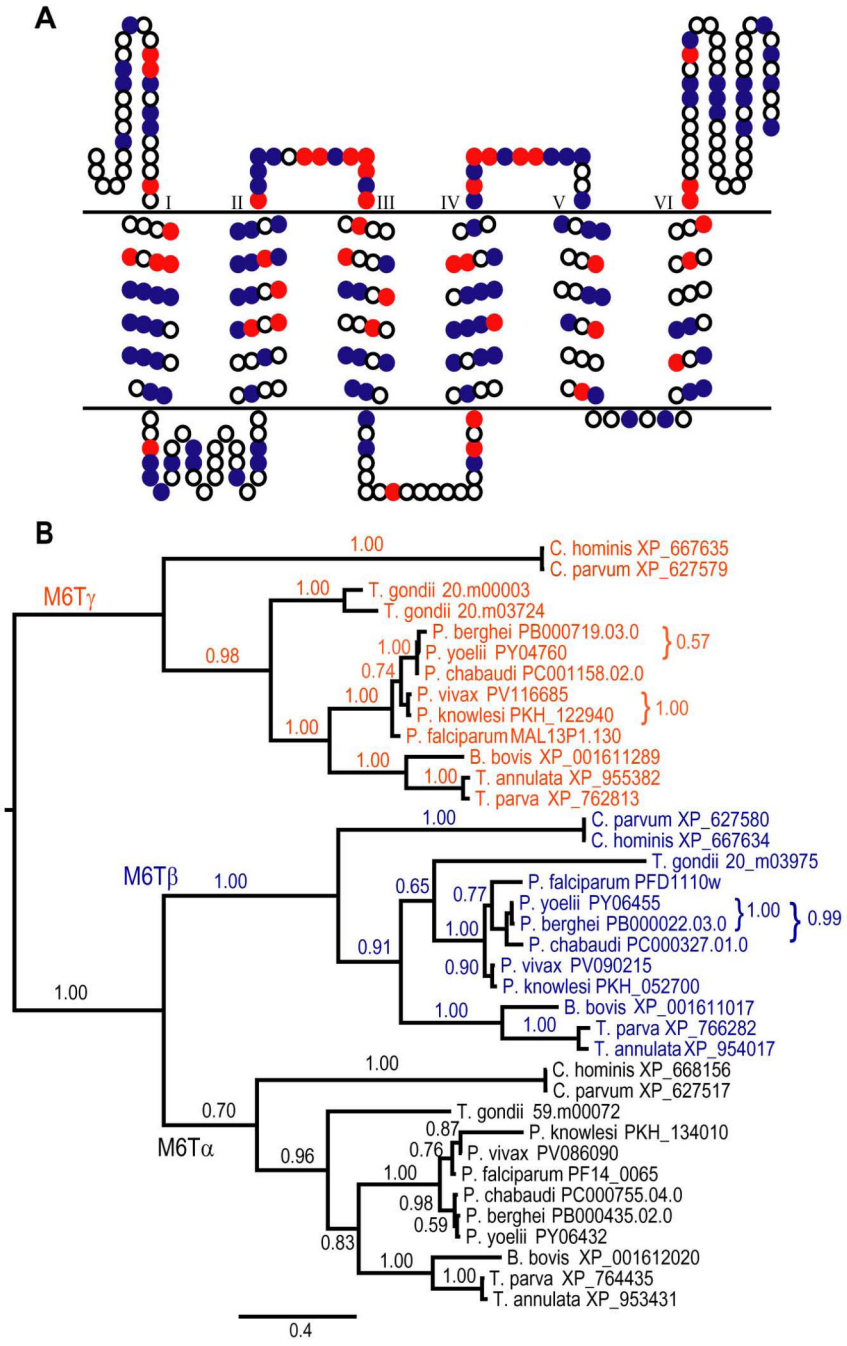

Fig. 1. Identification of the M6T family

(A) Membrane topology of PfM6Tα with each residue represented by a bead. The positions of the 6 predicted transmembrane domains, labeled with roman numerals, were determined using the TMHMM 2.0 algorithm. Residues conserved between the three *P. falciparum* paralogs are indicated using blue or red beads to represent identity between 2 or all 3 paralogs, respectively. (B) Unrooted Bayesian phylogeny of the apicomplexan M6T sequences. Posterior probabilities are given above or below the branches or using a curly bracket. The scale bar for branch lengths in this tree represents the number of expected changes per site [15]. Note the clear separation of the three paralogous clades.

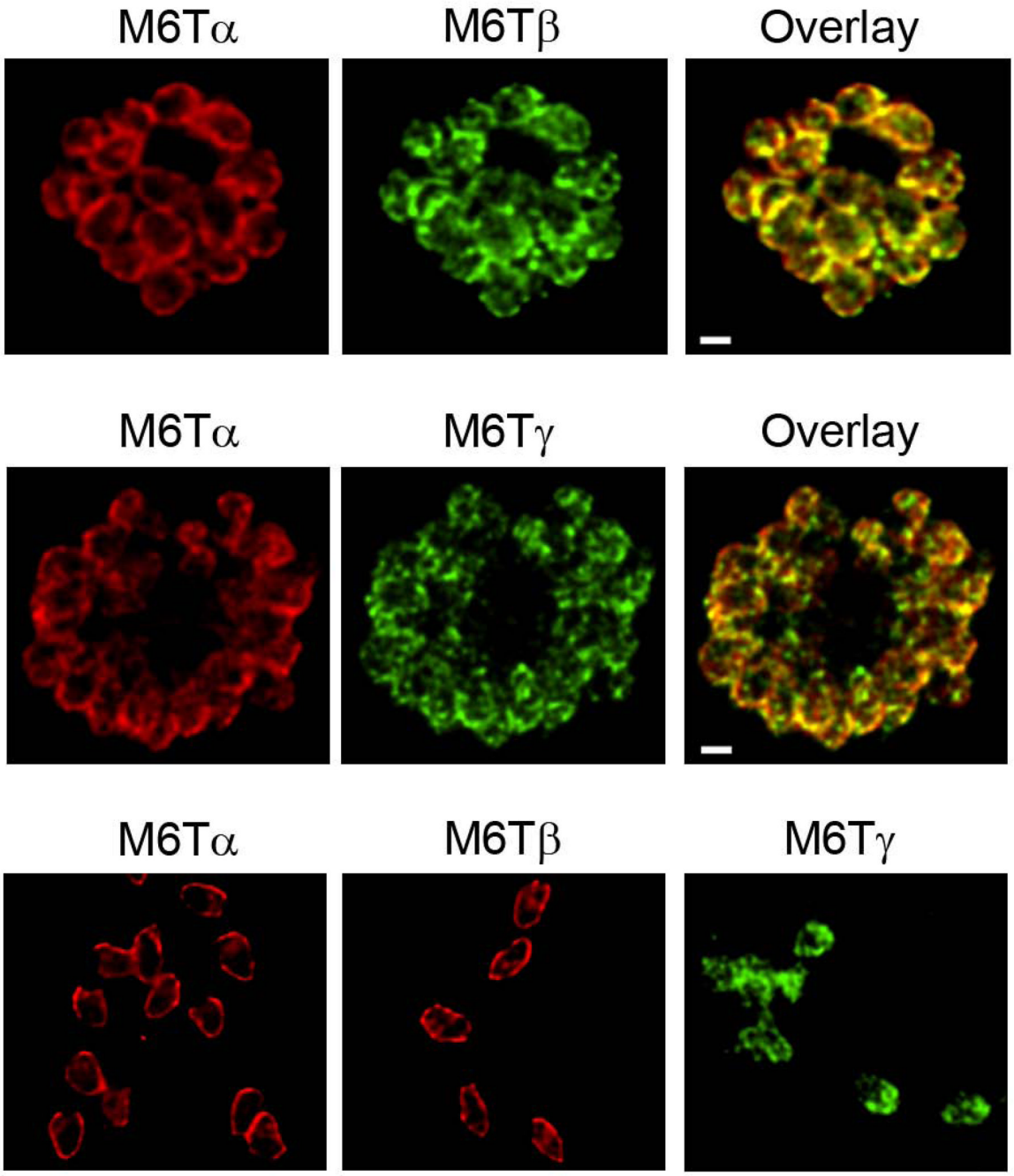

Fig. 2. PfM6T proteins localize to the merozoite IMC

Confocal immunofluorescence images demonstrating location of each paralog, as indicated above each image. The top two rows of images each show a separate schizont-infected erythrocyte containing many merozoites; overlay of the red and green channels (rightmost column) shows colocalization of PfM6Tα with each other paralog. The bottom row shows each protein's localization on spontaneously released merozoites. Red and green images reflect detection using specific antibodies raised in rabbits and mice, respectively. White scale bars represent 1 μM.

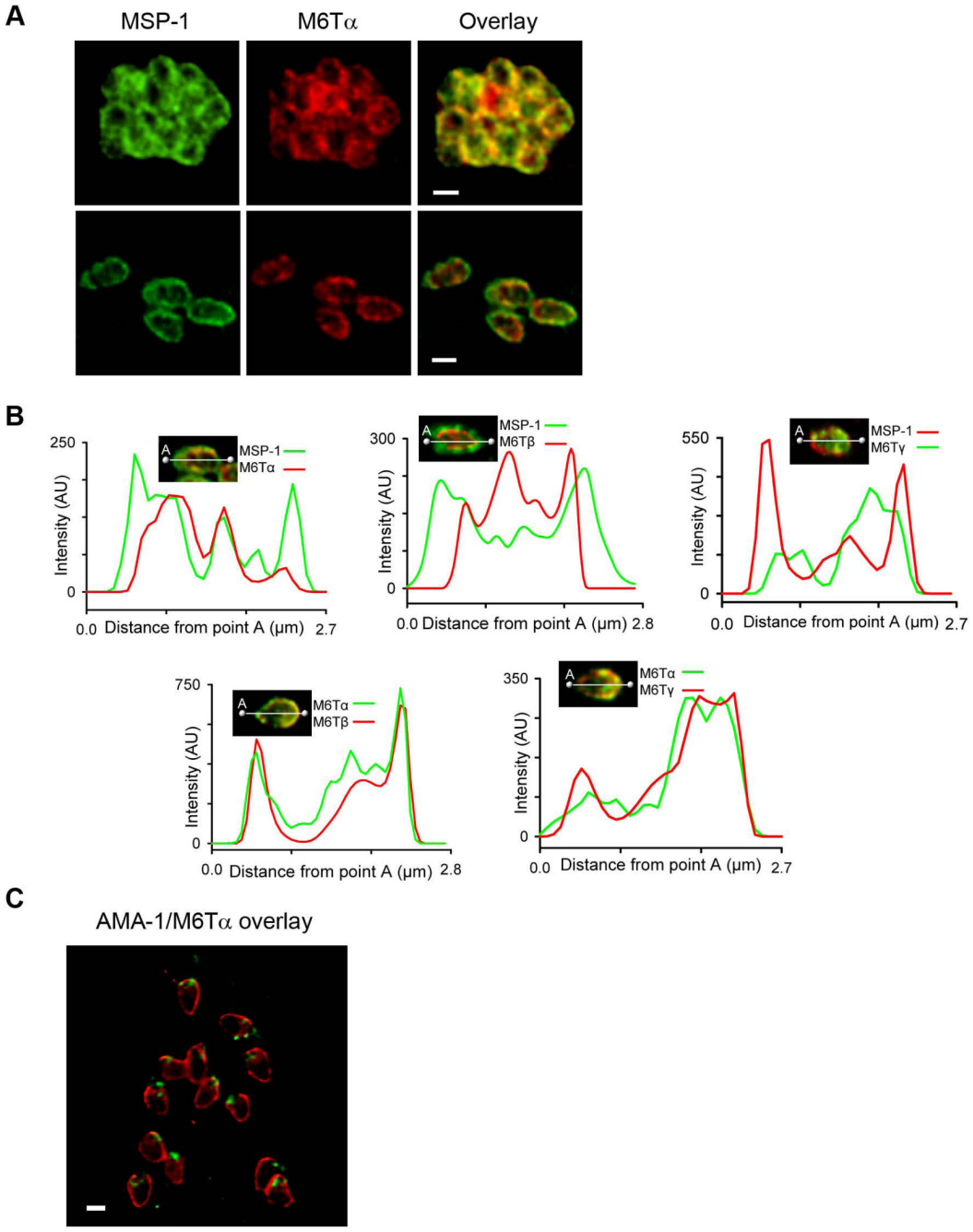

Fig. 3. PfM6T does not colocalize with MSP-1 or AMA-1

(A) IFA images of schizont-infected erythrocytes or freed merozoites (top and bottom rows, respectively) showing labeling with antibodies against PfM6Tα (*red*) and MSP-1 (*green*). Poor colocalization of these proteins is shown in the overlay of these images. (B) Quantification of label intensities along the parasite apical-posterior axis using single cells probed with two antigen-specific antibodies as indicated in each panel. Each *x-y* plot shows fluorescence intensity in arbitrary units at each point along the white line superimposed on the confocal image as a function of distance from point A. These positional intensities suggest that MSP-1 is external to each of the PfM6T proteins, which colocalize with each other precisely. (C) Freed merozoites demonstrating AMA-1 is restricted to the apical end of merozoites (*green*), but that

PfM6Tα has a diffuse surface distribution (*red*). There is reduced PfM6Tα labeling at the apical end of each cell (overlay). Scale bars in *A* and *C* represent 1 μm. Similar results were obtained for PfM6Tβ and PfM6Tγ (not shown).

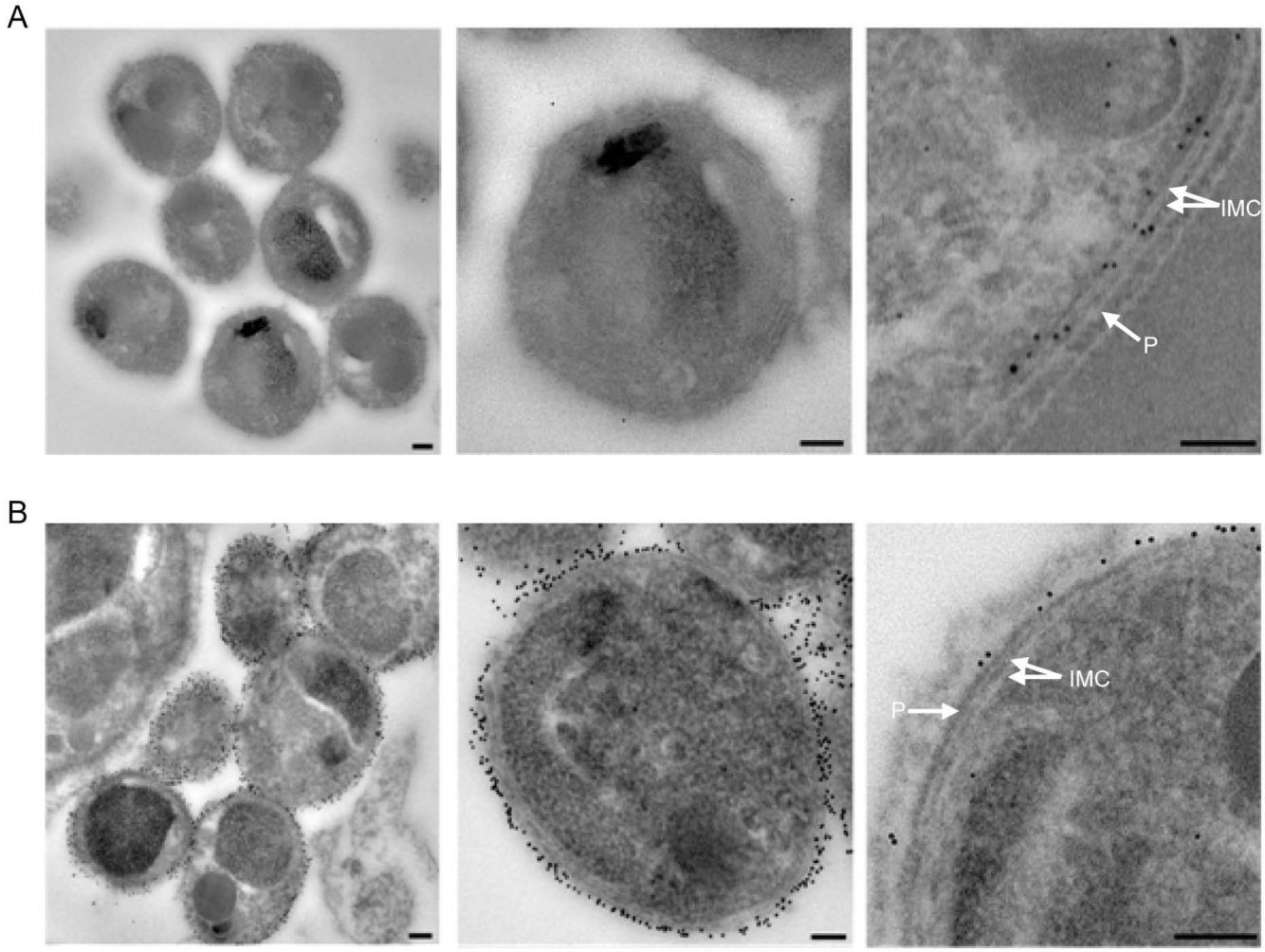

Fig. 4. PfM6T proteins localize on the IMC

Immuno-electron micrographs of merozoites probed with antibodies against PfM6Tα or MSP-1 (A and B, respectively) and detected with secondary antibodies conjugated to nanogold particles. In each row, the first two images were obtained with pre-embed antibody labeling of intact merozoites, while the rightmost image used antibodies applied after embedding and sectioning to permit access to intracellular antigens. Note that MSP-1 is recognized on intact merozoites, whereas PfM6Tα is not. Sectioning shows MSP-1 is on the parasite plasma membrane while PfM6Tα is on the IMC. Black scale bars in each image represent 100 nm. IMC, inner membrane complex; P, parasite plasma membrane.

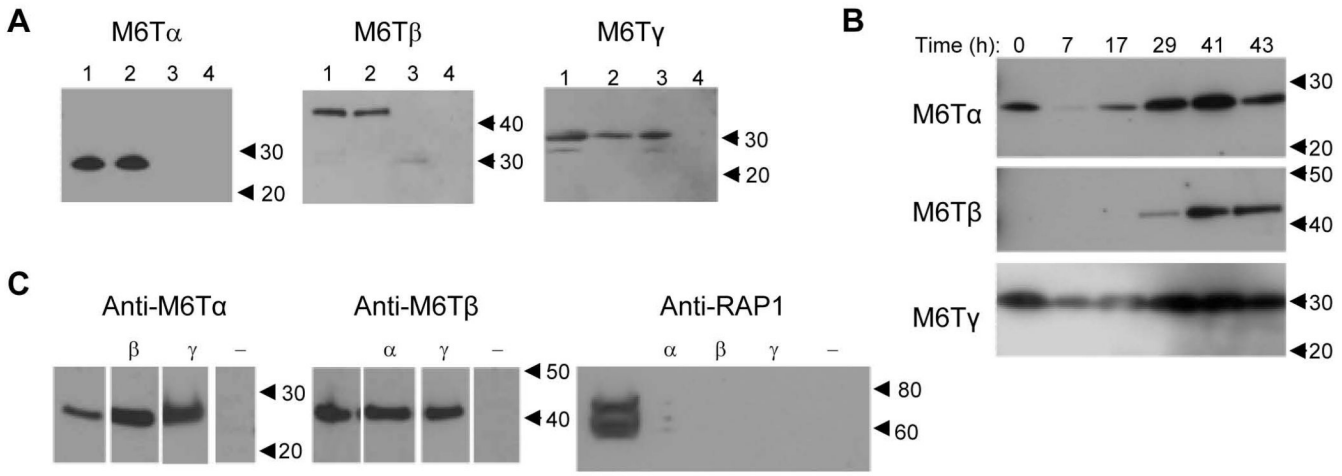

Fig. 5. PfM6T proteins are simultaneously expressed and form a heterocomplex

Immunoblots showing specific detection of each PfM6T paralog as indicated above each group. In each group, lanes 1–3 were prepared from infected erythrocytes as a total lysate (lane 1), membrane fraction (lane 2), and soluble fraction (lane 3). Lane 4 corresponds to a total lysate prepared from uninfected erythrocytes. (B) Stage specific expression of each paralog, determined using immunoblots of parasite membranes harvested at indicated timepoints in h after synchronization. Each protein is maximally expressed on schizonts and merozoites. (C) Immunoblots demonstrating co-precipitation of each paralog with PfM6Tα and PfM6Tβ (first and second groups) and not with RAP1 (third group). The first lane in each group is a control that shows blotting of total infected cell lysate without precipitation. Subsequent lanes reflect protein eluted from beads conjugated to antibodies against indicated paralog or without antibodies ("—"). Positions of molecular weight standards (in kDa) are indicated to the right of each blot.

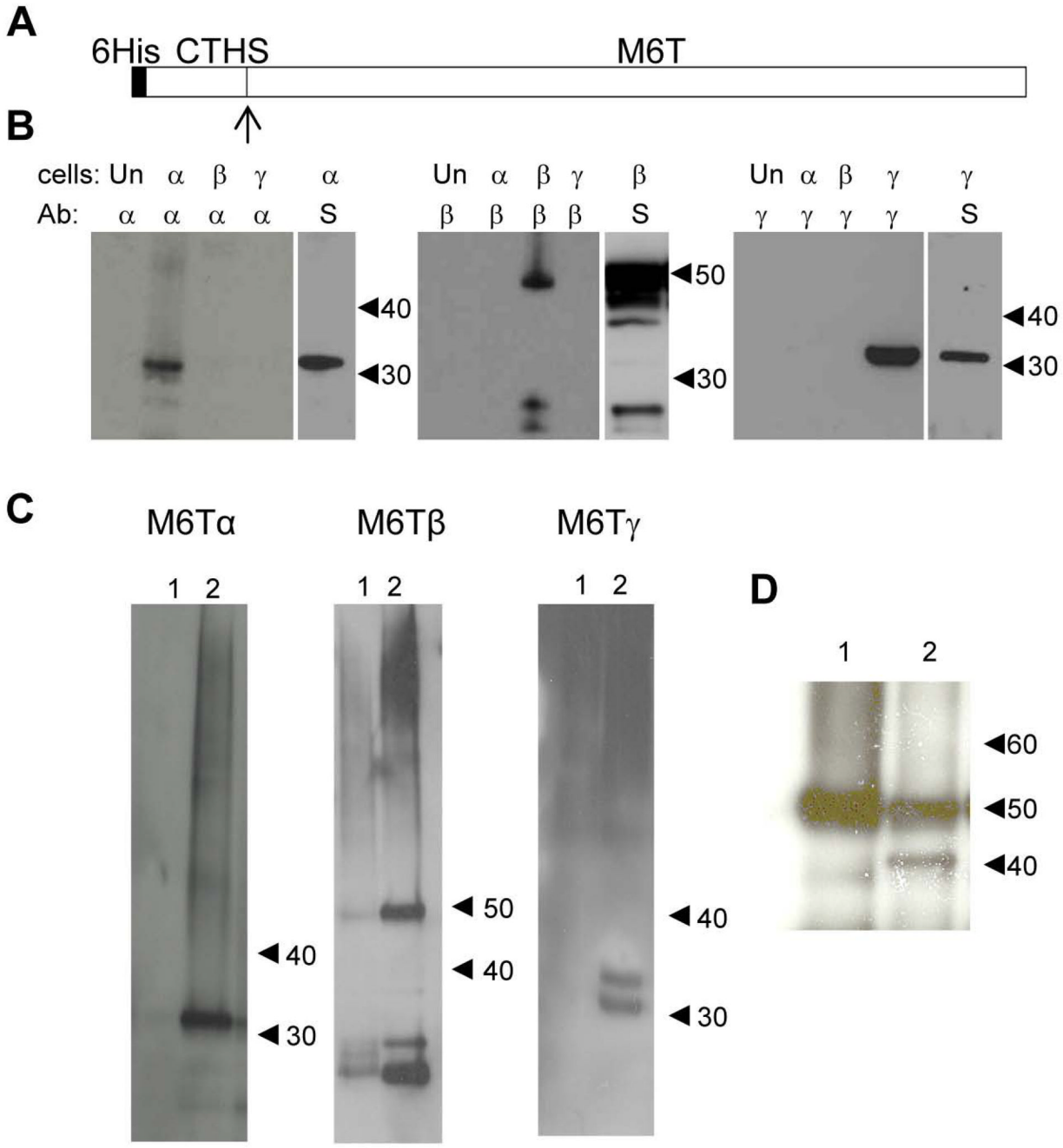

Fig. 6. Expression on insect cells

(A) Schematic representation of the engineered chimeric protein. The N-terminal tag (6-His followed by a 53 residue CTHS) increases the expected molecular weight of the fusion protein by approximately 6 kDa. This tag can be removed by SUMO protease digestion (arrow). (B) Immunoblots showing detected expression of each 6-His-CTHS-PfM6T chimera. In each group, total lysate from untransfected Sf9 cells ("Un") or from transfected cells that express a single PfM6T paralog as indicated in the top row above each blot was loaded and probed with either paralog-specific antibody or anti-SUMO antibody recognizing the CTHS tag ("S", bottom row above blot). Each specific antibody recognizes only cells expressing the corresponding protein. (C) Immunoblots showing reconstitution of expressed proteins,

enriched by Ni^{2+}-NTA purification from *T. ni* extracts, into azolectin liposomes (lane 2). In each blot, an ultracentrifugation supernatant (lane 1) revealed negligible amounts of soluble protein. (D) Liposome-reconstituted PfM6Tβ before and after cleavage of the 6-HIS-CTHS tag by SUMO protease to yield the native PfM6Tβ (lanes 1 and 2, respectively). The molecular weight of the cleaved protein is 42 kDa, matching that of the *in situ* parasite protein. The positions of molecular weight standards (in kDa) are indicated to the right of each blot.

Table 1

Properties of the *pfm6t* genes.

gene ID	product name	predicted MW (kDa)	peak expression[a] (h)	% similarity (identity)[b] to PfM6T α	% similarity (identity)[b] to PfM6Tβ
PF14_0065	PfM6Tα	32.8	47	-	-
PFD1110w	PfM6Tβ	42.4	47	56 (32)	-
MAL13P1.130	PfM6Tγ	33.8	47	43 (27)	40 (22)

[a] Peak expression is based on genome-wide expression microarrays for the 3D7A isolate and is presented in h after erythrocyte invasion [6].

[b] Similarity and identity are based on comparisons of predicted protein sequences after Clustal W alignment.